Available online at www.sciencedirect.com
ScienceDirect
Bioorganic & Medicinal Chemistry Letters 18 (2008) 2062–2066
Bioorganic & Medicinal Chemistry Letters

Structure-based design of novel groups for use in the P1 position of thrombin inhibitor scaffolds. Part 2: *N*-acetamidoimidazoles

Richard C. A. Isaacs,[a,*] Mark G. Solinsky,[a] Kellie J. Cutrona,[a] Christina L. Newton,[a] Adel M. Naylor-Olsen,[b] Daniel R. McMasters,[b] Julie A. Krueger,[c] S. Dale Lewis,[c] Bobby J. Lucas,[c] Lawrence C. Kuo,[d] Youwei Yan,[d] J. J. Lynch[e] and E. A. Lyle[e]

[a]*Department of Medicinal Chemistry, Merck Research Laboratories, West Point, PA 19486, USA*
[b]*Department of Molecular Systems, Merck Research Laboratories, West Point, PA 19486, USA*
[c]*Department of Biological Chemistry, Merck Research Laboratories, West Point, PA 19486, USA*
[d]*Department of Structural Biology, Merck Research Laboratories, West Point, PA 19486, USA*
[e]*Department of Pharmacology, Merck Research Laboratories, West Point, PA 19486, USA*

Received 1 November 2007; revised 14 January 2008; accepted 25 January 2008
Available online 30 January 2008

Abstract—Guided by X-ray crystallography of thrombin-inhibitor complexes and molecular modeling, alkylation of the N1 nitrogen of the imidazole P1 ligand of the pyridinoneacetamide thrombin inhibitor **1** with various acetamide moieties furnished inhibitors with significantly improved thrombin potency, trypsin selectivity, functional in vitro anticoagulant potency and in vivo antithrombotic efficacy. In the pyrazinoneacetamide series, oral bioavailability was also improved.

In a previous disclosure[1] we demonstrated that simple azoles and in particular, imidazoles, in spite of their relatively weak basicity ($pK_a \sim 7$) could be employed as the S1-binding element in the design of both noncovalent peptide and nonpeptide thrombin inhibitors by optimizing the proximity of the inhibitor's P1 imidazole nitrogen to the carboxylate of Asp189 in the thrombin active site. Additional potency enhancement was achieved by incorporating a methyl group on the imidazole, putatively in part by modestly increasing the basicity of the imidazole and also partly by making lipophilic contact with the aliphatic side chain of Val213. This strategy led to the development of pyridinone imidazole compound **1** (Fig. 1), a potent thrombin inhibitor ($K_i = 8$ nM) which is 5400-fold selective for thrombin versus trypsin ($K_i = 43$ μM). The functional in vitro anticoagulant potency of inhibitor **1** was assessed by measuring the concentration of the inhibitor required to double the activated partial thromboplastin time (APTT) in human plasma (1.1 μM).[2] It also performed poorly in vivo in the rat ferric chloride efficacy assay (3/6 animals occluded at an iv infusion rate of 10 μg/kg/min).[3] By comparison, the aminopyridine analog **2** (Fig. 1) is not only potent ($K_i = 0.5$ nM) and selective (6400-fold) for thrombin versus trypsin ($K_i = 3.2$ μM) but shows 5-fold higher functional anticoagulant activity in the 2× APTT assay (0.21 μM) and full in vivo efficacy in the rat ferric chloride assay (0/6 occlu-

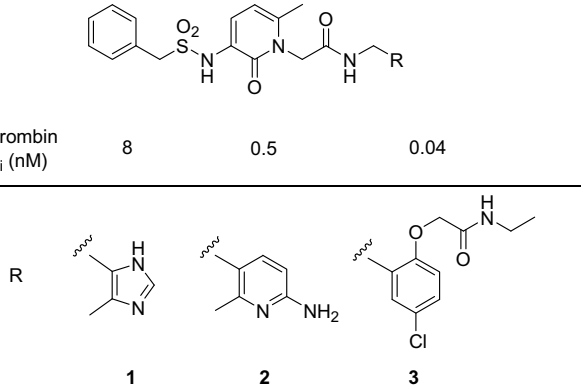

Figure 1. Comparison of binding potency of imidazole P1-bearing thrombin inhibitor **1** with analogs bearing more potent but structurally distinct P1 ligands.

Keywords: Thrombin; Anticoagulant.
* Corresponding author. Tel.: +1 215 652 0880; fax: +1 215 652 3971; e-mail: richard_isaacs@merck.com

0960-894X/$ - see front matter © 2008 Elsevier Ltd. All rights reserved.
doi:10.1016/j.bmcl.2008.01.098

sions at an iv infusion rate of 10 μg/kg/min).[4] The overall portfolio of properties embodied in inhibitor **2** made it attractive as a drug development candidate. However, the aminopyridine P1 ligand imparted unacceptable off target activity which the imidazole P1 ligand did not. We therefore sought to improve upon inhibitor **1**. In this paper we will describe how we used P1 targeted structure-based design techniques to further optimize **1**, the objective being to more closely match the mix of desirable activities and properties found in inhibitor **2**.

We first focused on improving binding potency and sought to take advantage of the wealth of enzyme–inhibitor X-ray structural information and molecular modeling data which we had generated in-house over time during our work on a number of different thrombin inhibitor scaffolds.

A detailed X-ray analysis of the potent methylaminopyridine inhibitor **2** bound to the α-thrombin–hirugen complex has been published.[4] For the purposes of the current discussion it is instructive to note that the methyl group of the methylaminopyridine points toward S1, making contact with the aliphatic side chain of Val213. The amino group makes a direct ionic interaction with the Asp189 carboxylate. An ordered water molecule forms a bridge between the pyridine nitrogen and the Asp189.

Previous disclosures from these laboratories have demonstrated that it is possible to design potent P1 ligands which bind without any ionic interaction with Asp189.[5] In particular, inhibitors such as **3** (Fig. 1) which contain a neutral 2,5-disubstituted benzylamine motif are very potent thrombin inhibitors. X-ray analysis of thrombin bound inhibitors bearing this P1 ligand[5b,c] revealed that the lack of a direct binding interaction with Asp189 is completely compensated for by the presence of hydrogen bonding interactions between the oxyacetamide moiety and the N—H of Gly219 on the thrombin β sheet. In principle, this seminal finding when combined with the X-ray data from inhibitor **2** offered a potentially attractive approach to improving the potency of the imidazole series through incorporating an acetamide residue onto the imidazole ring.

An overlay of the bound crystal structures of inhibitors **2** and **3** with an active site model of inhibitor **1** indicated that there were two potential sites for incorporation of an acetamide moiety onto the imidazole, namely N1 and C4 (Fig. 2). Based on this analysis we initially proposed hybrids **4** and **5** for consideration. Prior to initiating any actual synthetic work, molecular modeling studies were carried out on proposed hybrids **4** and **5**, the minimized structures each being compared in turn to the X-ray structures of inhibitors **2** and **3** and the active site model of **1**. In so doing it was determined that because of the smaller internal 108 degree bond angle of an imidazole (as in the imidazole P1 of inhibitor **1**) relative to the larger internal 120° bond angle of a benzene ring (as in the phenyl P1 of inhibitor **3**), a methyl group attached to imidazole (at either N1 or C4) occupies approximately the same region of space as the methylene group in the oxyacetamide portion of the 2-phenoxyacetamide in **3**. This led to a further refinement

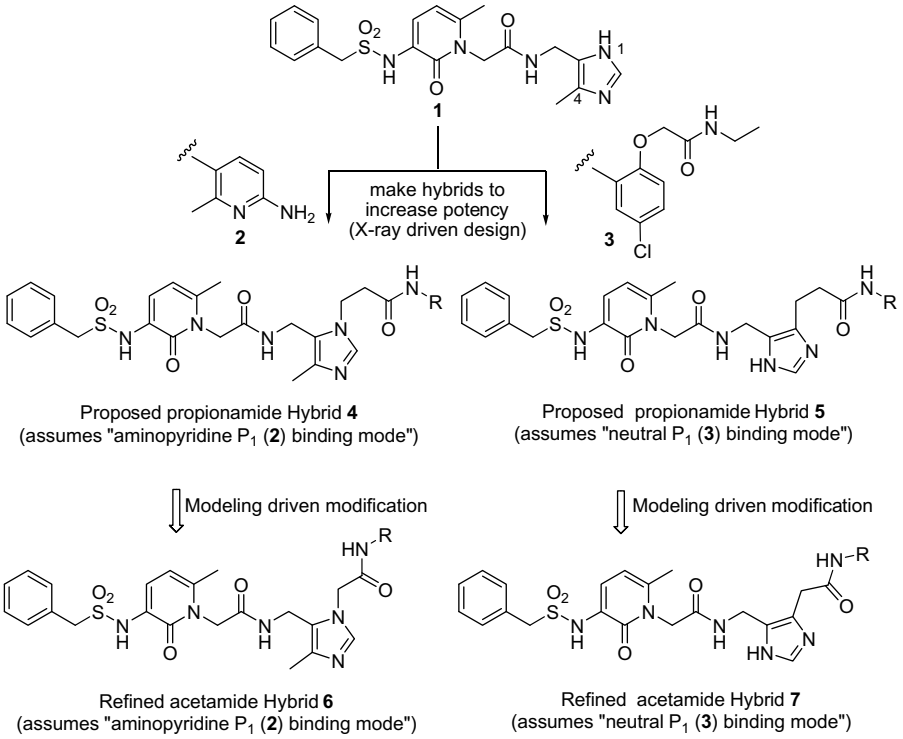

Figure 2. Proposed X-ray inhibitor-complex structure driven modification of the imidazole portion of inhibitor **1** targeting increased binding affinity for thrombin.

of our proposed hybrids from **4** and **5**, respectively, to **6** and **7**. We chose to test our hypothesis first with hybrid **6** as opposed to hybrid **7** because the chemistry to make N-alkylated imidazoles was more straightforward than the chemistry to make C-alkylated imidazoles.

The synthesis of hybrid **6** type compounds proceeded as outlined in Figure 3.[6] Alkylation of 5-methylimidazole-4-methanol **8** with *tert*-butyl bromoacetate gave a 2:1 mixture of alkylated isomers **9a** and **9b** which were separable by column chromatography. The regiochemistry of the major alcohol isomer **9a** was confirmed by NOE studies on a subsequent derivative. Alcohol **9a** was converted to azide **10** which was then reduced to amine **11**. Amine **11** was incorporated into the pyridinone scaffold via standard amide coupling to give the imidazole-*N*1-acetate **12**. We were gratified to find that **12**, an intermediate towards the first compound in our proposed series of alkylated imidazoles was a very potent thrombin inhibitor (K_i = 0.48 nM), 16-fold more potent than the parent imidazole **1** (K_i = 8 nM), and equipotent with the methylaminopyridine **2** (K_i = 0.5 nM) whose overall activity profile was being targeted. Ester **12** was converted to acid **13** (K_i = 31 nM) which was then parlayed into a number of different amides (Table 1). Alternatively, removal of the *tert*-butyl group from the intermediate azide **10**, coupling to an appropriate amine, reduction of the azide and subsequent coupling to the pyridinone acid also provided access to these *N*-acetamidoimidazole hybrid analogs.

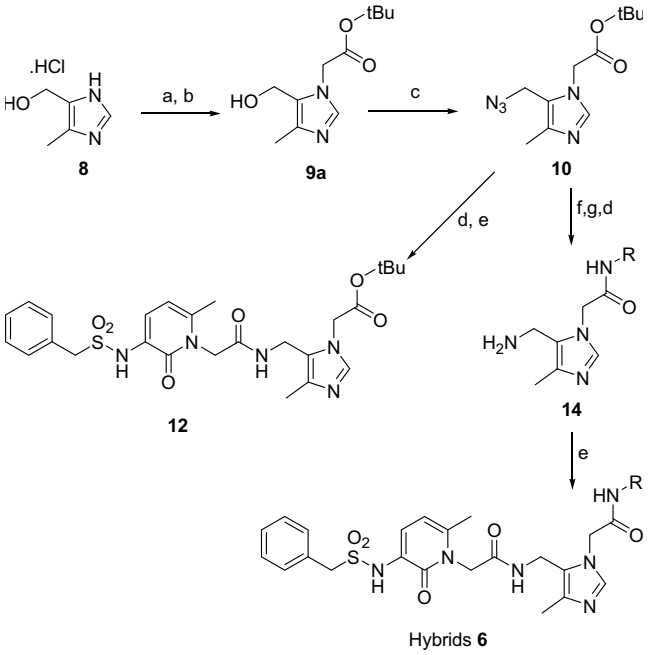

Figure 3. Synthesis of hybrids **6** and analog **12**. Reagents and conditions: (a) $BrCH_2CO_2tBu$, K_2CO_3, DMF; (b) chromatographic separation; (c) $(PhO)_2PON_3$, DBU, DMF; (d) H_2, 10% Pd/C, EtOAc; (e) RCO_2H, EDC, HOBt, Et_3N, DMF; (f) HCl, EtOAc, 0 °C; (g) RR′NH, EDC, HOBt, Et_3N, DMF.

Relative to the unalkylated imidazole lead **1**, the imidazoleacetamides as a class are very potent (low and sub-nanomolar) thrombin inhibitors which show a high degree of tolerance for structural diversity (lipophilic, hydrophilic, cyclic, and acyclic substituents) at the amide position. This is in contrast to the original neutral phenoxyacetamide series exemplified by **3** where only small lipophilic amides (e.g., ethyl and cyclopropyl) were tolerated.[5b]

Another improvement over the unalkylated imidazole **1** is that the imidazoleacetamide class of inhibitors is uniformly very highly selective for thrombin versus trypsin (>40,000-fold). This high degree of selectivity is also ob-

Table 1. Thrombin and trypsin inhibition constants, in vitro anticoagulant potency, and in vivo antithrombotic efficacy for compounds **12** and **15**–**29**

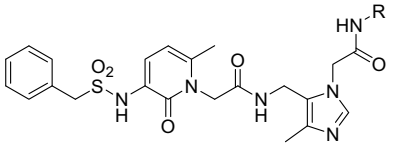

Compound	R	Thrombin K_i (nM)	Trypsin K_i (μM)	Fold selectivity	2× APTT (μM)	$FeCl_3$
12	*t*-Bu ester	0.48	50	104,000	ND	4/6
15	*t*-Bu	0.36	68	190,000	0.52	2/6
16	Et	2	137	70,000	0.7	4/6
17	*c*-Pr	1.8	185	103,000	0.68	ND
18	*c*-$PrCH_2$	1.1	57	52,000	0.53	ND
19	$EtCMe_2$–	0.19	34	180,000	0.56	ND
20	CF_3CH_2	0.83	49	59,000	0.53	1/6
21	Morpholine	1.9	101	53,000	0.51	ND
22	4-HO-azetidine–	2.8	167	48,000	0.66	ND
23	$HOCH_2CH_2$	2.4	115	48,000	0.85	ND
24	$H_2NCH_2CH_2$	0.9	85	94,000	0.39	0/6
25	4-Piperidine	0.65	56	86,000	0.37	0/6
26	3-Piperidine	0.31	110	355,000	0.35	0/6
27	$H_2NCH_2CMe_2$–	0.3	70	233,000	0.32	ND
28	4-H_2N-azetidine–	3	122	41,000	0.65	ND
29	$H_2NCMe_2CH_2$–	0.68	80	118,000	0.26	ND

served relative to the full panel of plasma and intestinal lumen proteases against which our thrombin inhibitors are routinely counter-screened (factor Xa, chymotrypsin, tPA, *p*-Kal).

Generally speaking, increased intrinsic thrombin potency, results in improved in vitro functional potency in the 2× APTT anticoagulant assay and in vivo efficacy in the rat ferric chloride efficacy model. However, this trend is often attenuated by physical properties such as protein binding and solubility.[7]

The performance of the imidazoleacetamide class of inhibitors in the 2× APTT functional clotting assay was significantly improved (routinely < 1 μM) relative to unalkylated imidazoles such as **1** (2× APTT = 1.1 μM) regardless of the nature of the amide moiety. Analogs in which the amide moiety contained polar functionality (e.g., **26** and **27**) displayed highest functional potency. This is consistent with prior observations that increasing polarity and hence higher plasma free fraction, confers increased functional anticoagulant potency.[7] Several analogs (again, particularly the ones such as **24** and **26** having more polar amides) displayed full efficacy in the rat ferric chloride antithrombotic assay. This trend is also consistent with prior observations.[7]

The X-ray crystal structure of **15** bound to the α-thrombin–hirugen complex was determined (Fig. 4) and provided partial validation for our molecular modeling-driven approach to improving binding potency. The benzylsulfonamidopyridinone moiety of the inhibitor occupies the S3 and S2 pockets of the enzyme as previously detailed.[4,5a,b] However, the key binding interactions in the S1 specificity pocket, while somewhat different from what was predicted based on modeling, still provided grounds for rationalization of the observed increase in binding potency. Additional productive hydrogen bonding interactions with the enzyme are indeed made. However, the S1 binding mode of the imidazole-*N*-acetamide in **15** is different from that of the noncharged oxyacetamide ligand in **3** in that the amide carbonyl of **15** makes a hydrogen bond to a nitrogen of Glu192 instead of Gly219. This 180° reversal then allows the acetamide NH to participate in hydrogen bonding to an ordered water molecule that also hydrogen-bonds to the nitrogen of Gly219 and the oxygen of Gly216. The *tert*-butyl group is still able to fill the lipophilic S4 pocket. However, with this mode of access, the S4 substituent is partially solvent exposed thereby allowing accommodation of more structurally diverse groups (hydrophilic as well as hydrophobic) unlike in the original phenoxyacetamide series where the S4 substituent is more deeply buried in the S4 pocket and tolerant of small hydrophobic groups.

Another view of the X-ray structure of **15** bound to thrombin (Fig. 5) demonstrates that the unalkylated nitrogen atom of the imidazole binds to the carboxyl of Asp189 via an ordered water molecule. In our previous paper[1] where we described the development of unalkylated imidazole inhibitor **1**, we noted that in the absence of a crystal structure of **1** bound to thrombin, active site modeling suggested that the imidazole group while being geometrically incapable of directly binding to Asp 189 was likely capable of doing so via an ordered water molecule. We had based that supposition on the imidazole–water–Asp189 interaction seen here with inhibitor **15**.

Having achieved significant improvements in intrinsic thrombin potency, trypsin selectivity, in vitro functional anticoagulant potency, and in vivo antithrombotic efficacy, we turned our attention to an evaluation of oral bioavailability in this series of inhibitors. Inhibitor **2** when dosed orally in dogs at 5 mpk displayed the following pharmacokinetic parameters: C_{max} = 5.31 μM,

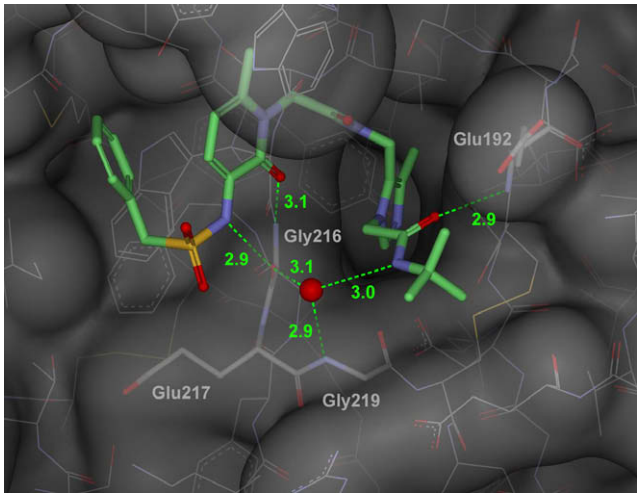

Figure 4. X-ray crystal structure of inhibitor **15** bound to the active site of human α-thrombin showing key hydrogen bonding S1 interactions with the imidazoleacetamide moiety (see Ref. 10).

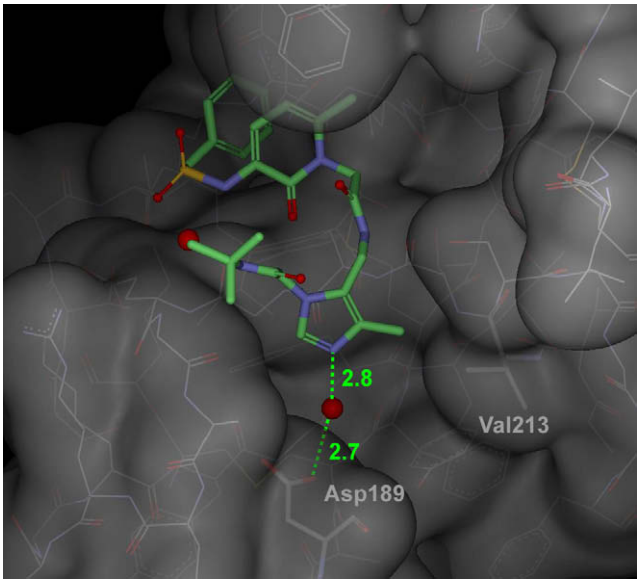

Figure 5. X-ray crystal structure of inhibitor **15** bound to the active site of human α-thrombin showing a water-mediated interaction of the imidazole nitrogen with the Asp189 carboxylate (see Ref. 10).

$t_{1/2}$ = 2.5 h, AUC = 18.8 μM h. By comparison, optimized *N*-acetamidoimidazole inhibitors such as **26** showed no oral absorption at the same dose. Although the bulk of this optimization was carried out in the pyridinone P2 series of inhibitors, while this work was in progress, modifications to the aminopyridinone core directed toward improving metabolic stability and oral bioavailability were under investigation. This effort led to the development of the aminopyrazinone template.[8] The piperidino-acetamidoimidazole P1 group present in **26** was incorporated into the aminopyrazinone scaffold. The resulting inhibitor **30** had an attractively balanced overall activity profile (thrombin K_i = 1.2 nM, trypsin K_i = 18 μM, 2× APTT = 0.7 μM, full efficacy in the rat ferric chloride assay, 0/6 occlusions at 10 μg/kg/min) albeit not as good as **26** but had better pharmacokinetic profile in dogs at an oral dose of 5 mpk (C_{max} = 1.46 μM, $t_{1/2}$ = 1.6 h) and rhesus monkeys, also at an oral dose of 5 mpk (C_{max} = 0.36 μM, $t_{1/2}$ = 1.1 h). None of these compounds however surpassed compound **2** in terms of full in vitro and in vivo profiles.[9]

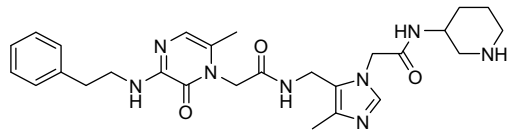

30

To summarise, by taking advantage of X-ray crystallographic data generated from a 'non-charged P1' series of thrombin inhibitors, we have further refined our series of imidazole P1 thrombin inhibitors. The resulting *N*-acetamidoimidazole inhibitors are very potent, selective and efficacious anticoagulants. Oral bioavailability thus far has been observed only in conjunction with our P3P2 pyrazinone scaffold.

Acknowledgment

We express our gratitude to John Wai, Neville Anthony and Thomas Tucker for helpful discussions during the preparation of this manuscript.

References and notes

1. Isaacs, R. C. A.; Solinsky, M. G.; Cutrona, K.; Newton, C. L.; Naylor-Olsen, A. M.; Krueger, J. A.; Lewis, S. D.; Lucas, B. J. *Bioorg. Med. Chem. Lett.* **2006**, *16*, 338.
2. We consider human plasma 2× APTT values of 1 μM or less to be generally predictive of good in vivo efficacy with lower concentrations being predictive of greater efficacy. We use this 1 μM mark routinely as a gate for determining whether to evaluate a compound further in vivo in the rat ferric chloride efficacy assay (see Ref. 3). In practice, in optimizing compounds, we strive to achieve 2× APTT values of <0.5 μM.
3. (a) Kurz, K. D.; Main, B. W.; Sandusky, G. E. *Thromb. Res.* **1990**, *60*, 269; (b) Lewis, S. D.; Ng, A. S.; Lyle, E. A.; Mellott, M. J.; Appleby, S. D.; Brady, S. F.; Stauffer, K. J.; Sisko, J. T.; Mao, S.-S.; Veber, D. F.; Nutt, R. F.; Lynch, J. J., Jr.; Cook, J. J.; Gardell, S. J.; Shafer, J. A. *Thromb. Haemostasis* **1995**, *74*, 1107; (c) In a typical experiment, six rats are evaluated. Full efficacy is defined as when none of the animals occlude i.e., 0/6 occlusions.
4. Sanderson, P. E. J.; Cutrona, K. J.; Dorsey, B. D.; Dyer, D. L.; McDonough, C.; Naylor-Olsen, A. M.; Chen, I.-W.; Chen, Z.; Cook, J. J.; Gardell, S. J.; Krueger, J. A.; Lewis, S. D.; Lin, J. H.; Lucas, R. J.; Lyle, E. A.; Lynch, J. J.; Stranieri, M. T.; Vastag, K.; Shafer, J. A.; Vacca, J. P. *Bioorg. Med. Chem. Lett.* **1998**, *8*, 817.
5. The following references are particularly germane to the subject matter at hand: (a) Lumma, W. C.; Witherup, K. M.; Tucker, T. J.; Brady, S. F.; Sisko, J. T.; Naylor-Olsen, A. M.; Lewis, S. D.; Freidinger, R. M. *J. Med. Chem.* **1998**, *41*, 1011; (b) Tucker, T. J.; Brady, S. F.; Lumma, W. C.; Lewis, S. D.; Gardell, S. J.; Naylor-Olsen, A. M.; Yan, Y.; Sisko, J. T.; Stauffer, K. J.; Lucas, B. J.; Lynch, J. J.; Cook, J. J.; Stranieri, M. T.; Holahan, M. A.; Lyle, E. A.; Baskin, E. P.; Chen, I. W.; Dancheck, K. B.; Krueger, J. A.; Cooper, C. M.; Vacca, J. P. *J. Med. Chem.* **1998**, *41*, 3210; (c) Sanderson, P. E. J.; Cutrona, K. J.; Dyer, D. L.; Krueger, J. A.; Kuo, L. C.; Lewis, S. D.; Lucas, B. J.; Yan, Y. *Bioorg. Med. Chem. Lett.* **2003**, *13*, 161.
6. For full experimental details, see: Isaacs, R. C. A.; Naylor-Olsen, A. M.; Dorsey, B. D.; Newton, C. L. PCT Intl. Appl. WO 9842342 A1, 1998.
7. Tucker, T. J.; Lumma, W. C.; Mulichak, A. M.; Chen, Z.; Naylor-Olsen, A. M.; Lewis, S. D.; Lucas, R.; Freidinger, R. M.; Kuo, L. C. *J. Med. Chem.* **1997**, *40*, 830.
8. Sanderson, P. E. J.; Lyle, T. A.; Cutrona, K. J.; Dyer, D. L.; Dorsey, B. D.; McDonough, C. M.; Naylor-Olsen, A. W.; Chen, I-W.; Chen, Z.; Cook, J. J.; Cooper, C. M.; Gardell, S. J.; Hare, T. R.; Krueger, J. A.; Lewis, S. D.; Lin, J. H.; Lucas, B. J.; Lyle, E. A.; Lynch, J. J.; Stranieri, M. T.; Vastag, K.; Yan, Y.; Shafer, J. A.; Vacca, J. P. *J. Med. Chem.* **1998**, *41*, 4466.
9. The in vitro profile of compound **2** was presented at the beginning of the manuscript. When dosed orally in dogs at 1 mpk the observed C_{max} was 1 μM and the $t_{1/2}$ was 2.5 h). For the corresponding aminopyrazinone analog, the in vitro profile was as follows: thrombin K_i = 0.8 nM, trypsin K_i = 1.8 μM, 2× APTT = 0.41 μM, full efficacy in the rat ferric chloride assay, 0/6 occlusions at 10 μg/kg/min. When dosed orally in dogs at 0.5 mpk the observed C_{max} was 2 μM and the $t_{1/2}$ was 3.8 h).
10. The X-ray coordinates for inhibitor **15** have been deposited with the RCSB Protein Data Bank database (Deposition No. 3C1K).